

A NUMERICAL MODELING FOR NATURAL CONVECTION HEAT TRANSFER IN POROUS MEDIA WITH GENERATED INTERNAL HEAT SOURCES

G. Karimi, M. Taheri and M. A. Yaghoubi

School of Engineering
Shiraz University
Shiraz, Iran

Abstract In this paper a numerical method is used to study the unsteady state natural convection heat transfer within a confined porous media with uniform internal heat generation. The governing equations based on the Darcy model and Bossinesq approximations are solved, using the finite difference Alternating Direction Implicit (ADI) method. The developed program was used to simulate natural convection heat transfer within the grain silos, where the respiration of the grains generates heat as a result of metabolism of the products. The results of the analysis show that for short periods (up to 40 days) natural convection is not the dominant heat transfer mechanism and the maximum temperature is on the centerline. In longer periods (greater than two months), fluid recirculation enhances and a cold region near the central axis of the silo is created due to natural convection.

چکیده در این مقاله با استفاده از روش عددی انتقال حرارت از طریق جابجایی آزاد، محیط‌های متخلخل با منبع گرمایی داخلی یکنواخت مورد مطالعه قرار گرفته است. معادلات حاکم در انتقال حرارت و حرکت سیال، براساس مدل دارسی (Darcy) و تقریب‌های بوزینسک (Bossinesq Approximations) بدست آمده و با استفاده از روش تفاضل محدود (ADI) حل شده‌اند. صحت برنامه کامپیوتری تهیه شده با بررسی انتقال حرارت در اشکالی که حل دقیق آنها دردسترس می‌باشد مطالعه و تأیید گردیده و سپس برنامه مذکور برای آنالیز انتقال حرارت از طریق جابجایی آزاد در سیلوهای ذخیره‌ای غلات که در آنها در اثر متابولیسم دانه‌ها، گرما تولید میشود مورد استفاده قرار گرفته است. نتایج بدست آمده نشان میدهد که در زمانهای کوتاه (کمتر از ۴۰ روز) جابجایی آزاد هوانمیتواند مکانیزم غالب انتقال حرارت باشد. در طول این مدت حداکثر درجه حرارت بر روی محور سیلو واقع میشود. در زمانهای طولانیتر (بیش از دو ماه) سرعت جابجایی هوای محبوس از میان دانه‌ها، باعث میگردد تا انتقال حرارت از طریق جابجایی آزاد قابل ملاحظه شود و موقعیت حداکثر درجه حرارت از محور به سمت سطوح جانبی در فاصله بین مرکز و دیواره جابجا گردد.

INTRODUCTION

Natural convection in porous media induced by internal heat generation arises in various physical problems such as heat removal from nuclear reactors, underground disposal of radioactive waste materials and exothermic chemical reactions in packed bed reactors. Numerous studies have been reported dealing with the numerical simulation of natural convection in a porous medium contained within rectangular enclosures [1-4]. This paper is concerned with natural convection during the storage of agricultural products in silos. During the storage, wheat, corn or seeds of various plants generate heat as a result of metabolism of products. Storage of these agricultural products at about

0°C , normally provides an optimal condition for long periods.

Because of heat transfer between the silo wall and surrounding air, a horizontal temperature gradient is established and this in turn results a natural convection in the container. Unsteady natural convection directs air upward at the center and downward near the walls, hence this air circulation influences the temperature distribution within the container.

In the present work numerical simulation of the governing equations based on the Darcy model approximations is carried out using the ADI finite difference technique in a cylindrical coordinate system. The numerical model is tested for some common geometries for which

analytical solutions are available. Thermal and hydrodynamic structures of the enclosure are determined for various periods and the corresponding maximum temperature within the silo is plotted with respect to time. In addition, effects of several parameters such as heat generation rate and initial temperature of the products are studied to illustrate their effects on temperature of the seeds. The simulated model can be used to predict the cooling period of the products for any kind of grain storage.

Mathematical Formulation

The physical geometry considered is a cylindrical enclosure of diameter $2R$ and height H containing porous (Darcy) medium as shown in Figure 1. By making the Bossinesq approximation and assuming thermal equilibrium between fluid and matrix, for a homogeneous isotropic condition continuity, momentum and energy equations can be written as:

$$\frac{\partial V_z}{\partial z} = 0 \quad (1)$$

$$\frac{\Phi_1 \mu}{\rho_r} \left[\frac{\partial^2 V_z}{\partial r^2} + \frac{1}{r} \frac{\partial V_z}{\partial r} \right] - \frac{\mu}{K \rho_r} V_z + \beta (\bar{T} - T_r) g = \frac{\partial V_z}{\partial t} \quad (2)$$

$$\alpha_m \left[\frac{\partial^2 T}{\partial r^2} + \frac{1}{r} \frac{\partial T}{\partial r} \right] + \alpha_m \frac{\partial^2 T}{\partial z^2} - \alpha_r V_z \frac{\partial T}{\partial z} + \gamma = \frac{\partial T}{\partial t} \quad (3)$$

In the above equations an effective thermal diffusivity of solid-fluid mixture α_m is used for the porous medium.

Most silos are very tall, such that it is reasonable to assume end effects are negligible and V_z is independent of height. However, V_z is a function of r in a way that the net mass flow rate at any section along the z axis is zero.

Equation (2) shows that V_z is a function of r and t , which is due to the buoyancy forces

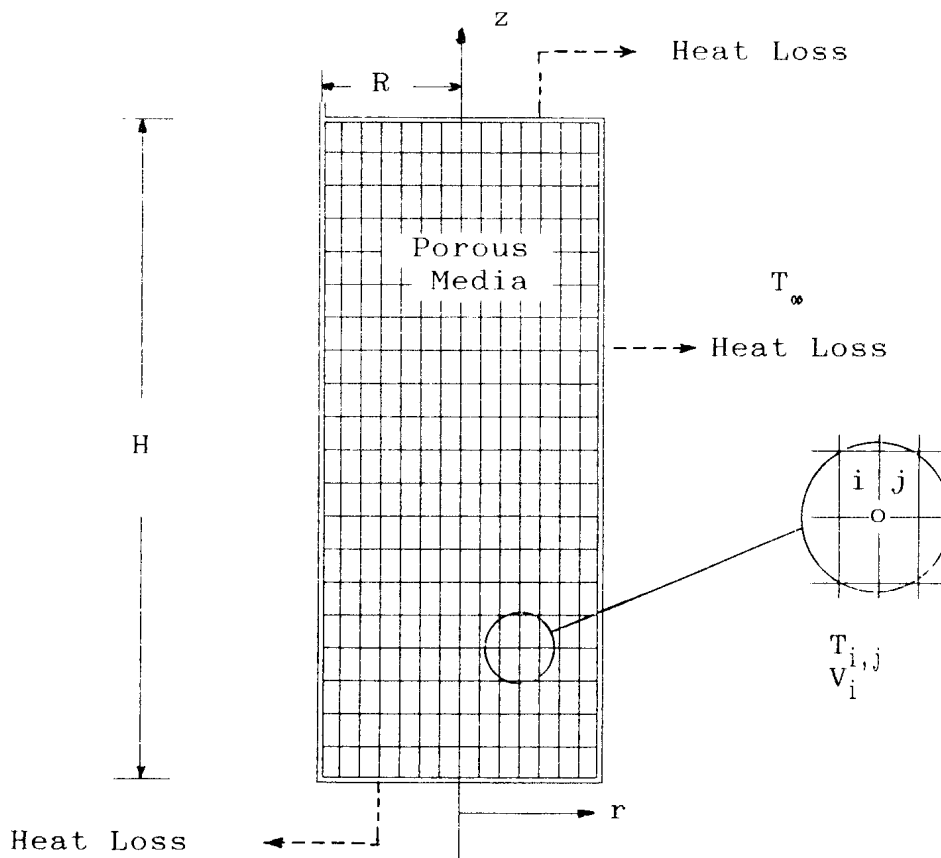


Figure 1. Cylindrical enclosure in mathematical modeling.

induced by temperature gradient. T_r is the reference temperature selected in such a way that the net flow rate at any cross section approaches zero. It is also assumed that due to symmetry about the centerline, the unsteady temperature of the grain is a function of r and z .

Also heat generation is assumed to be uniform within the container, but the generation rate can be different with respect to the kind of the agricultural products.

Boundary conditions and initial conditions of the problem are as follows:

For $t = 0$:

$$0 \leq r \leq R \quad V_z = 0 \quad (4)$$

$$0 \leq r \leq R, 0 \leq z \leq R \quad T = T_o \quad (5)$$

For $t \geq 0$:

$$r = 0 \quad \frac{\partial V_z}{\partial r} = 0 \quad (6)$$

$$r = R \quad V_z = 0 \quad (7)$$

$$r = 0, \text{ all } z \quad \frac{\partial T}{\partial r} = 0 \quad (8)$$

$$r = R, \text{ all } z \quad -K_{eff} \frac{\partial T}{\partial r} = U_{sw} \cdot \Delta T_{sw} \quad (9)$$

$$z = 0, \text{ all } r \quad -K_{eff} \frac{\partial T}{\partial r} = U_b \cdot \Delta T_b \quad (10)$$

$$z = H, \text{ all } r \quad -K_{eff} \frac{\partial T}{\partial r} = U_t \cdot \Delta T_t \quad (11)$$

Numerical Methods

The nonlinear coupled partial differential equations (2,3) are solved simultaneously by using implicit methods to avoid large time consumption in the computer calculations.

In solving the energy equation the ADI (Alternative Direction Implicit) procedure is used. This method was originally developed by Douglas and Peaceman [5] for conduction and adapted to natural convection enclosure problems by many investigators [6-8]. It has been shown that ADI methods which are an extension of the Crank-Nicholson scheme are stable for linear and mildly nonlinear parabolic and elliptic systems. In our study the solution is based on solving two different equations which are used in turn over successive time-steps of $\Delta t/2$. The first

set of equations is implicit only in the r direction and the second is implicit only in the z direction. Numerical solution of equation of motion is carried out by the simple implicit method. To obtain finite difference equations at each point of a grid all spatial derivatives were replaced by three point central difference approximation and the time derivative was replaced by forward difference approximations. For each column or row of the grids the corresponding set of equations form a tridiagonal matrix, which were solved by using Thomas algorithm [9].

For the calculation of buoyancy force in the equation of motion at each grid point a suitable local temperature must be selected. According to the slight temperature variation along the z axis, this local temperature is determined from the following relation:

$$\overline{T}_i = (\sum_j T_{1,j})/j \quad (12)$$

The truncation error associated with the central finite difference method is of order Δr^2 and Δz^2 and accuracy of the numerical solution is affected by the temperature gradient within the container. For sharp temperature gradients grid spaces must be reduced to avoid any significant errors. However, satisfactory convergence is achieved by using values of $\Delta r = 15$ cm, $\Delta z = 50$ cm and time step, $\Delta t = 8$ hr for period of 40 days of the enclosure operation.

RESULTS

The accuracy of the numerical formulation is tested for some common geometries for which analytical solutions are available. The models are:

a) Infinite cylinder without porosity and internal heat generation sources.

In this case, due to the lack of porosity, fluid flow is zero and according to the infinite length, there is no temperature gradient along the z direction. A scheme describing this situation is shown in Figure 2.

Under this condition equation (3) is simplified

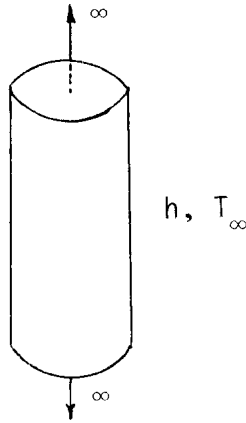


Figure 2. A schematic of an infinite cylinder.

to:

$$\alpha_m \left[\frac{\partial^2 T}{\partial r^2} + \frac{1}{r} \frac{\partial T}{\partial r} \right] = \frac{\partial T}{\partial t} \quad (13)$$

Analytical solution of equation (13) consists of Bessel's functions and is available in reference [10]. The analytical and numerical solution is based on information listed in Table, 1 and corresponding results are compared in Figure 3.

It can be seen that the finite difference method of solution can be used to predict

Table 1. Inputs for the Tested Model of an Infinite Cylinder

Parameters	Values
Thermal diffusivity	$2 \times 10^{-6} \text{ m}^2/\text{s}$
Thermal conductivity	$2 \text{ W/m} \cdot ^\circ\text{C}$
Heat transfer coefficient	$30 \text{ W/m}^2 \cdot ^\circ\text{C}$
Surrounding temperature	400°C
Initial temperature	20°C
Radius	10 cm

transient temperature distribution in the container in r direction with reasonable accuracy. Furthermore, this figure shows that any reduction in the node spacing results in higher accuracy of solution.

b) Finite cylinder, without porosity and heat generation sources.

This special case is shown in Figure 4.

Under this condition equation (3) is simplified to:

$$\alpha_m \frac{\partial^2 T}{\partial z^2} = \frac{\partial T}{\partial t} \quad (14)$$

Transient temperature distribution within the cylinder is determined by solving equation (14), and with parameters given in Table 2. Comparison of the analytical and numerical

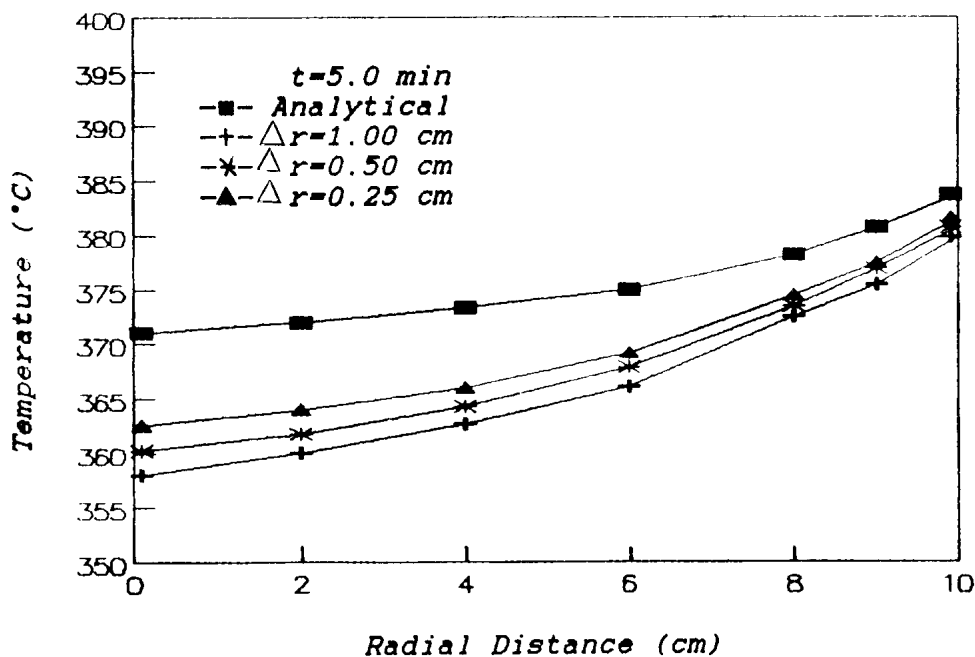


Figure 3. Comparison of numerical and analytical results in the case of infinite cylinder.

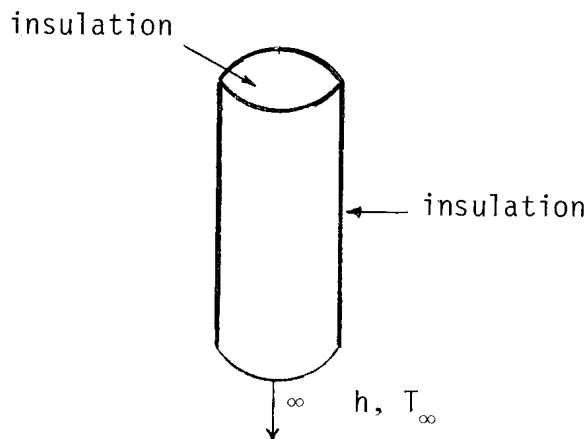


Figure 4. A schematic of an insulated finite cylinder.

Table 2. Inputs for the Tested Model of an Infinite Cylinder

Parameters	Values
Thermal diffusivity	$2 \times 10^{-5} \text{ m}^2/\text{s}$
Thermal conductivity	$2 \text{ W/m} \cdot ^\circ\text{C}$
Heat transfer coefficient	$50 \text{ W/m}^2 \cdot ^\circ\text{C}$
Surrounding temperature	$300 ^\circ\text{C}$
Initial temperature	$50 ^\circ\text{C}$
Height	50 cm

results is presented in Figure 5. This figure shows that the selected finite difference method has adequate accuracy in predicting temperature

distribution. Also it can be found that where the temperature gradient is nearly zero, mesh size has no effect on the accuracy of the numerical solution. For the present conditions, because of a slight temperature gradient with respect to position and time, relatively large node spacing and time intervals can be selected whereas adequate accuracy and a stable numerical solution will be obtained.

The model was also tested for several other geometrics and very good results were obtained [11].

In order to study thermal and hydrodynamic structure of a grain silo, a typical container in Shiraz is selected with parameters given in Table 3.

Table 3. Specification of an Actual Grain Silo in Shiraz

Parameters	Values
Height of container	50.0 m
Diameter	9.2 m
Overall heat transfer coef.	$5.0 \text{ W/m}^2 \cdot ^\circ\text{C}$
Grain thermal diffusivity	$1 \times 10^{-7} \text{ m}^2/\text{s}$
Grain thermal conductivity	$0.25 \text{ W/m} \cdot ^\circ\text{C}$
Heat generation rate	15.0 W/m^3
Porosity	35%
Permeability	0.0001 m^2

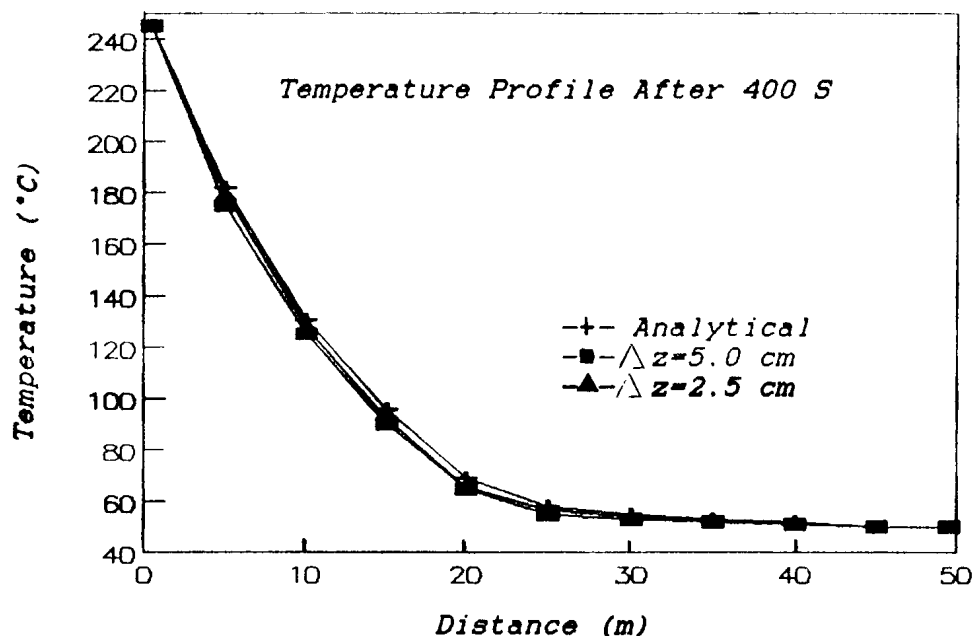


Figure 5. Comparison of numerical and analytical results in the case of an insulated finite cylinder.

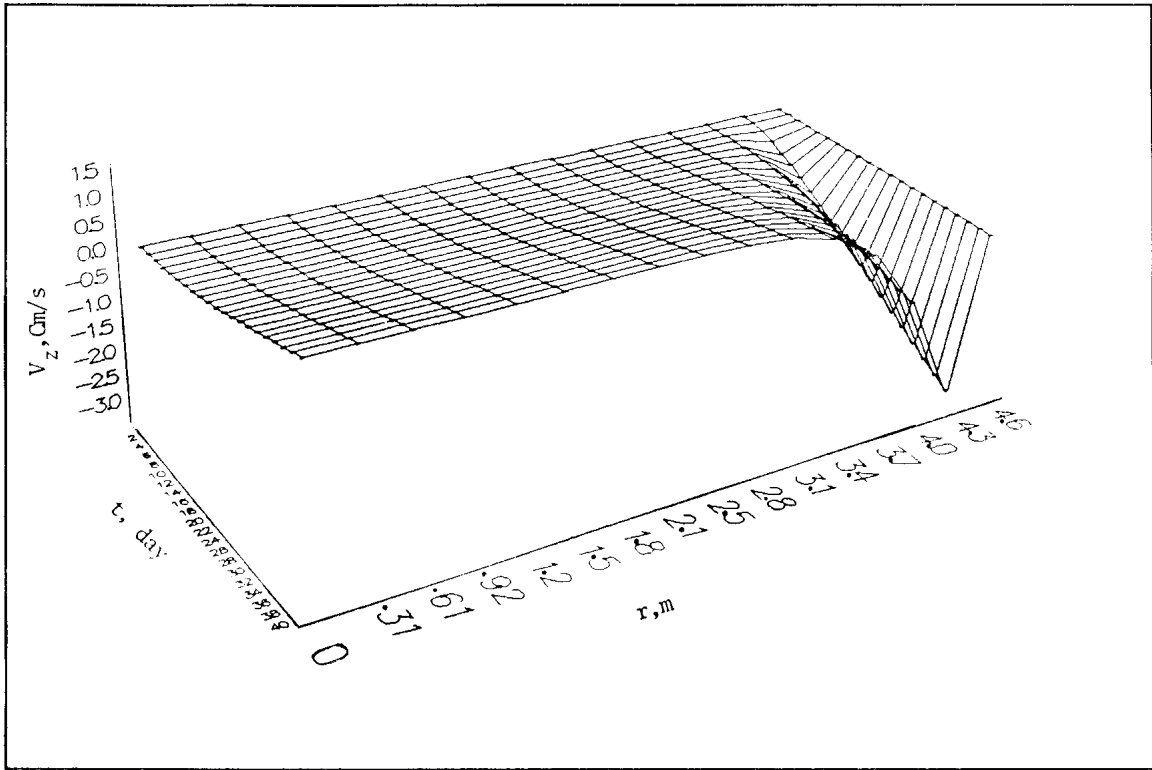


Figure.6: Typical velocity distribution in the grain silo during several days.

$[T_o = T_\infty = 25.0 \text{ }^\circ\text{C}, U = 5.0 \text{ W/m}^2 \cdot \text{ }^\circ\text{C}, Q = 15.0 \text{ W/m}^3]$

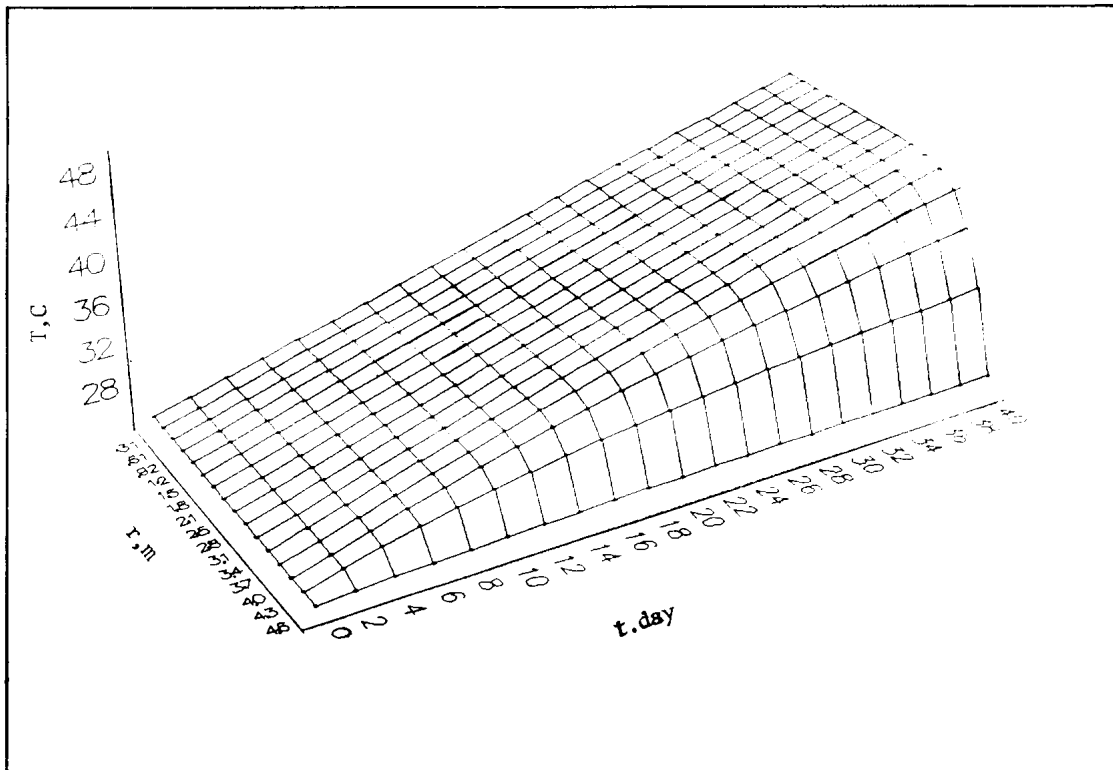


Figure 7. Typical temperature distribution in the grain silo during several days.

$[T_o = T_\infty = 25.0 \text{ }^\circ\text{C}, U = 5.0 \text{ W/m}^2 \cdot \text{ }^\circ\text{C}, Q = 15.0 \text{ W/m}^3]$

The data of the grain in Table 3 are based on measurements and overall heat transfer coefficient is determined for the silo with 20 cm thickness and outside convection coefficient of $20 \text{ W/m}^2 \cdot ^\circ\text{C}$ [11].

For this situation calculations were performed for several days of storage. During 1-40 days of operation a symmetrical flow is generated and the induced velocities within the enclosure are very small and heat transfer takes place mainly by conduction. Figures 6 and 7 show both velocity and temperature distribution across the cylinder with respect to time. Note, due to symmetry of flow with respect to centerline of the cylinder, only one-half of the cross section is shown. The flow is symmetric about the centerline, flowing upward at the center and moving downward near the cold wall, and due to the presence of the side wall, the velocity decreases rapidly near the wall. Temperature is high in the central part of the container and it is lower near the wall where heat transfer takes place by conduction to the wall. Bulk temperature rises linearly with respect to time and it is nearly uniform about the axis of the cylinder. The pattern of velocity and temperature

profiles remains the same unless the temperature gradient increases.

A numerical study is made to determine the influences of several parameters on thermal and hydrodynamic structure of the grain silo, such as surrounding environmental conditions, initial grain temperature, grains heat generation rate and finally grain types. Results are shown in Figures. 8-12.

Figures 8-10, show that surrounding conditions do not have considerable effect on the safe storage period because of the relatively low thermal diffusivities of grains. However, only after a very long period of time, a small portion close to the wall is affected.

Effect of initial grain temperature on the temperature distribution is shown in Figure 11, after 40 days of storage. Maximum temperature which is located in the central part, rises linearly with time for 40 days. The lower the initial temperature, the longer the safe storage period.

The most important factor affecting the thermal structure of the grains is the heat generation rate. Figure 12 presents maximum temperature in the silo with respect to the time for different heat generation rates. Note that

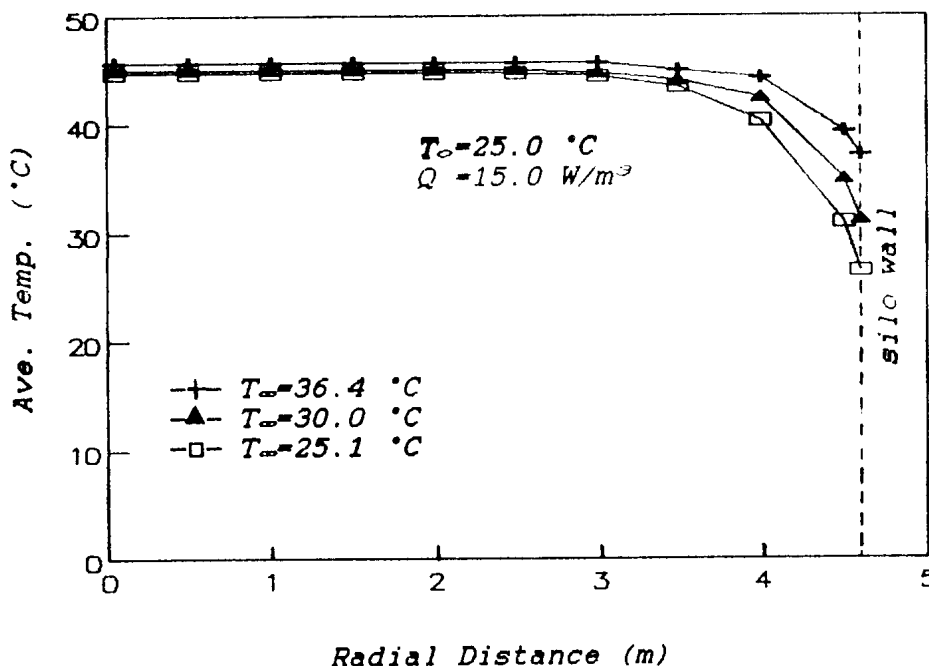


Figure 8. Effect of surrounding temperature on the temperature profile (after 40 days).

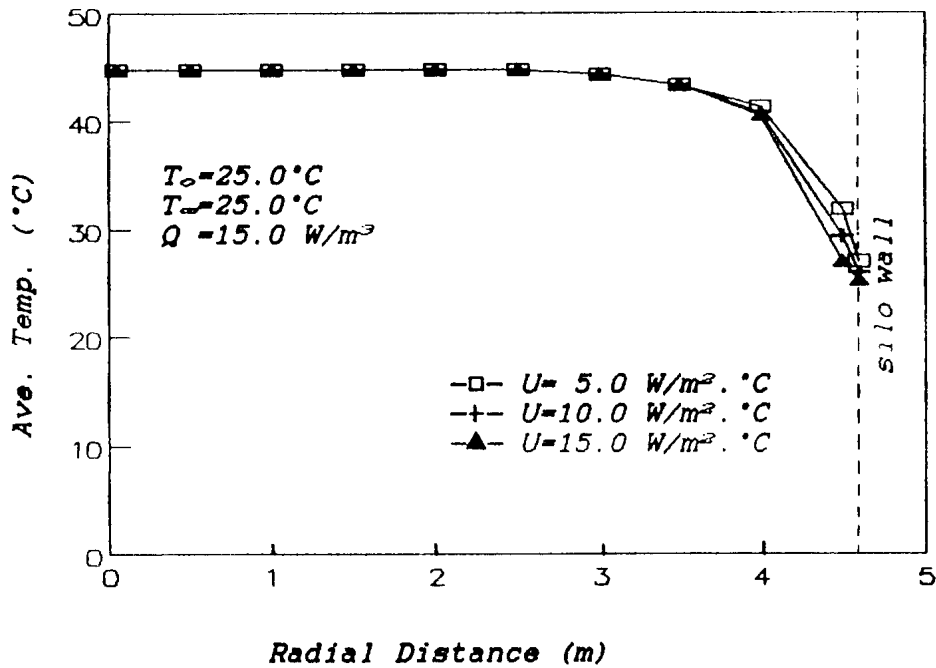


Figure 9. Effect of overall heat transfer coefficient on the temperature profile (after 40 days).

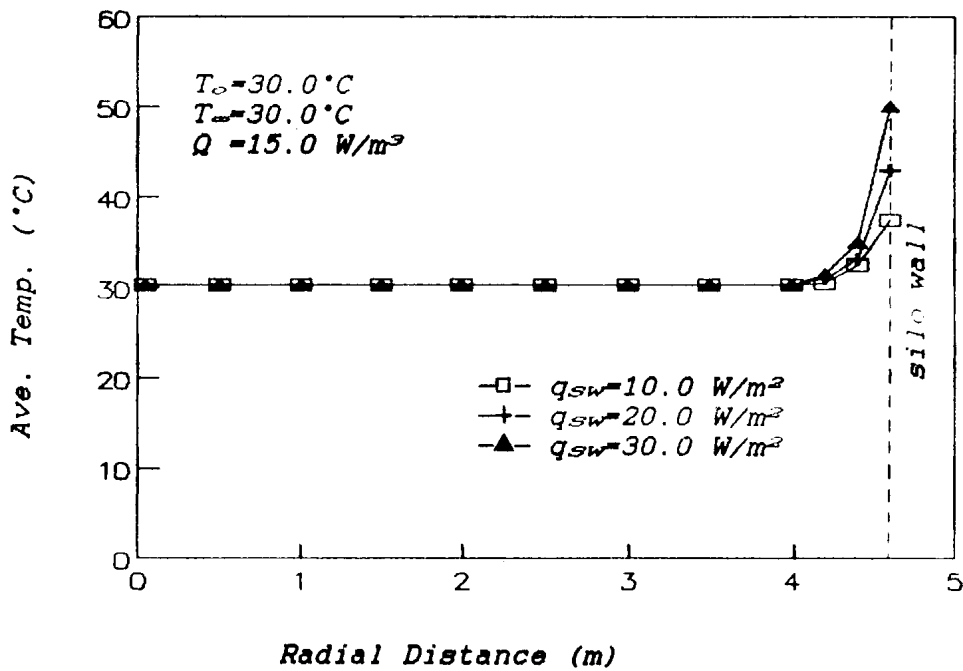


Figure 10. Effect of radiation fluxes on the temperature profile (after 16 hours).

heat generation increases with grain humidity. Humidity causes the lypase enzyme within the grains to be activated and the corresponding rate of respiration reactions to be increased. As a result of this exothermic reaction, heat is evolved and bulk temperature of the grains also

increases, Hence, one procedure for safe storage is control of humidity of grains and possible drying before storage.

Grain storage for long periods exhibits different thermal structure within the enclosure. For long periods, temperature rises further and

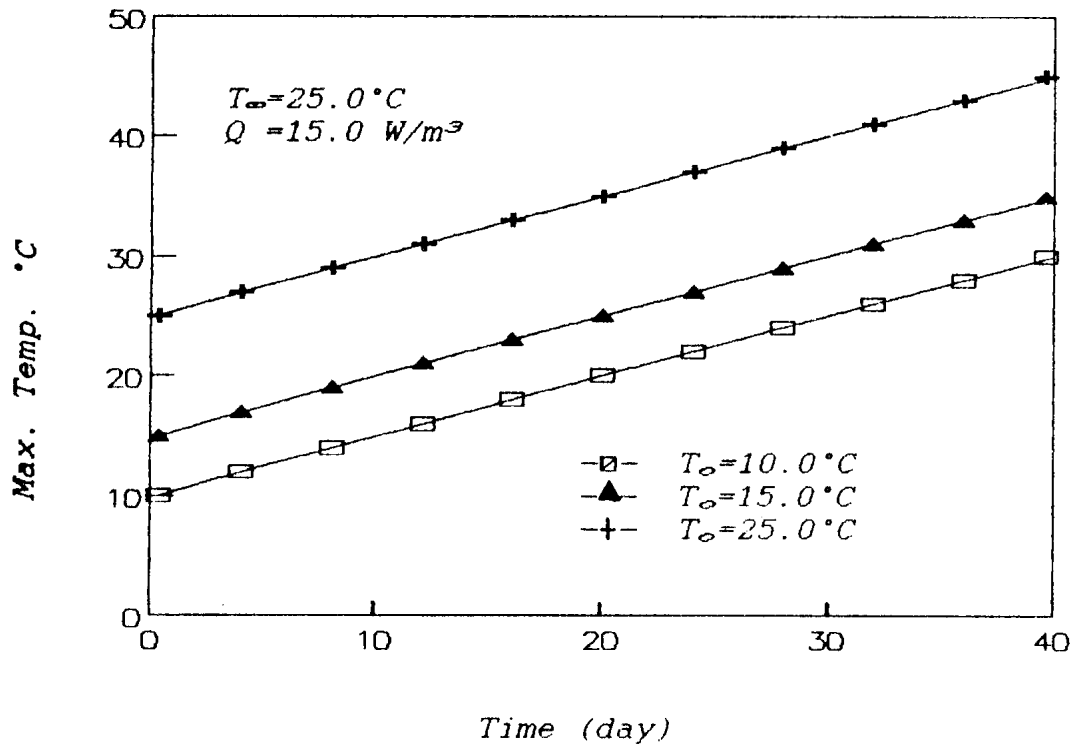


Figure 11. Effect of initial storage temperature on the temperature profile.

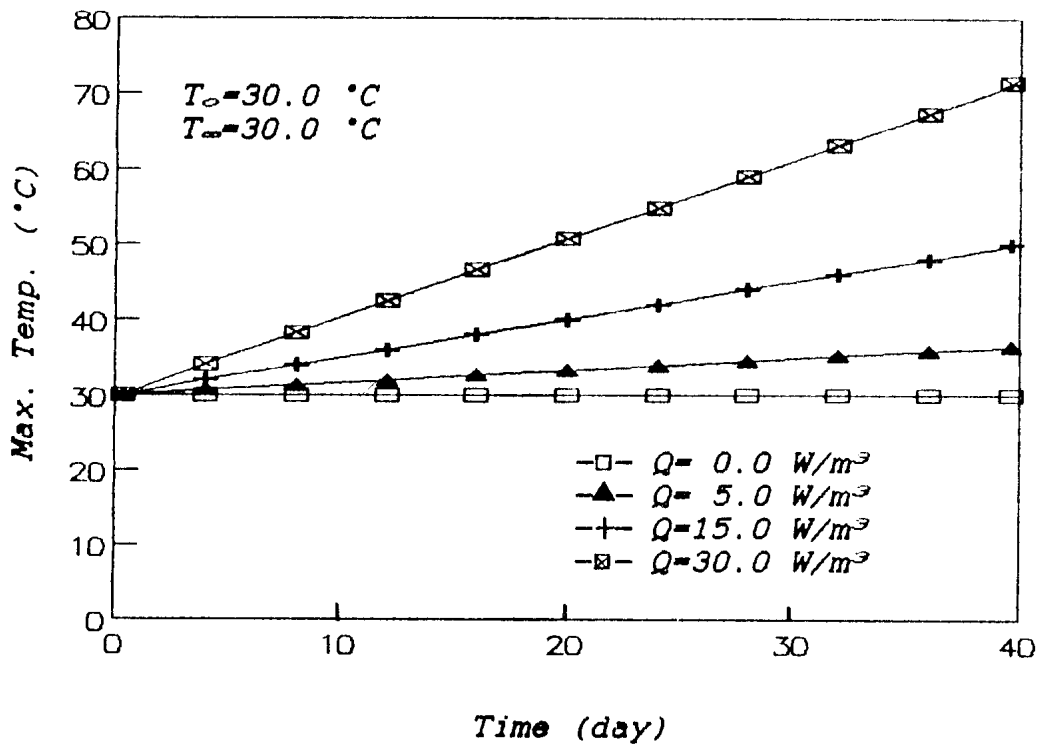


Figure 12. Effect of generation rate on the temperature profile.

induced air velocity increases too, hence, air circulation is not weak and heat transfer in the cavity is no longer dominated by conduction.

With high temperature gradient in radial coordinate, convection heat transfer increases in the central part and near the wall of the

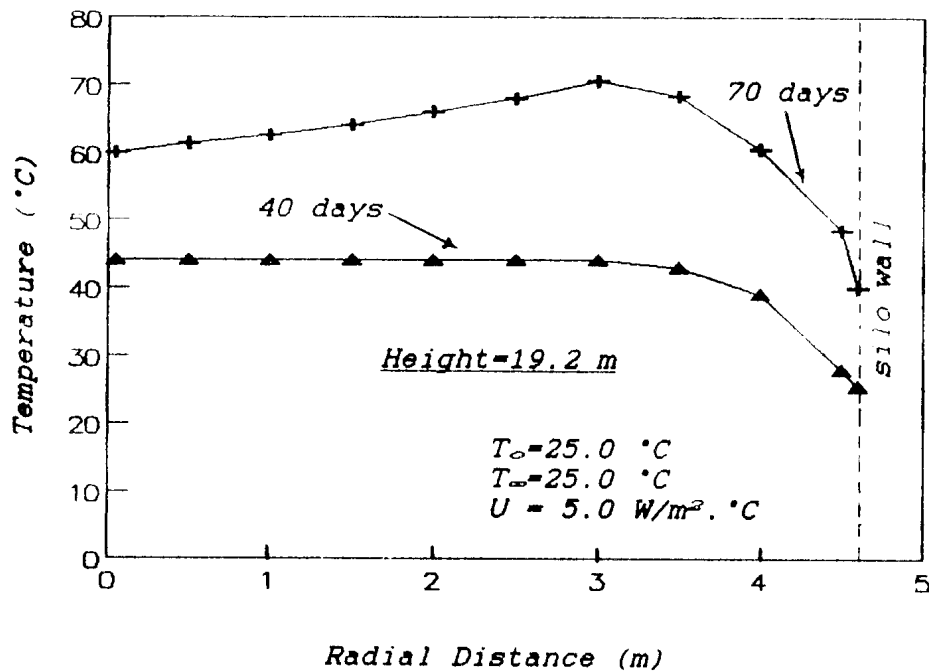


Figure 13. Temperature distribution for long periods.

container. However, in the region of about $R/\sqrt{2}$, velocity is zero and consequently, conduction heat transfer is predominant and grain temperature is maximum in this region as shown in Figure 13.

In long periods of storage (more than two months) numerical solution shows oscillatory behavior at the top while the bottom is stable. This is due to the fact that in the upper section, temperature of the ceiling is relatively lower and hence denser than the confined fluid under it. This behavior indicates that the numerical solution should be modified for very long periods of storage by including two dimensional variation of fluid velocity in the container.

CONCLUSION

A numerical simulation of natural convection heat transfer in a grain silo with heat generation rate was made to analyze transient thermal and hydrodynamic structure of the porous medium for different periods. It is found that the model is stable for the periods when vertical temperature gradient is negligible. For short periods, about 40 days, heat transfer is mainly

by conduction and maximum temperature appears at the center of the container, while for longer periods, i.e. 70 days, air circulation enhances and the hottest region shifts to about $R/\sqrt{2}$, where fluid velocities are about zero.

From the various parameters affecting thermal structure of the grains, initial grain temperature and heat generation rate have direct influence on shortening the safe storage period of grain while boundary conditions are negligible.

However numerical simulation can be used as a tool to predict the period for a safe storage of any kind of grain in silo with reasonable accuracy.

NOMENCLATURE

C_p	average heat capacity
g	acceleration due to gravity
H	height of silo
K	permeability
K_{eff}	effective thermal conductivity
Q	heat generation rate
r	radial distance
t	time
T	temperature

\bar{T}	average temperature at any radial point
T_r	reference temperature
U	overall heat transfer coefficient
V	induced velocity

Greek letters

β	thermal expansion coefficient
μ	fluid viscosity
ρ	fluid density
Φ	porosity
Φ_s	sphericity

Relations

$$\alpha = (\rho C_p)_a / (\rho C_p)_m$$

$$\alpha_m = K_{eff} / (\rho C_p)_m$$

$$\Upsilon = Q / (\rho C_p)_m$$

$$\Phi_1 = [1 + (2(1 - \Phi)) / \Phi \cdot \Phi_s]$$

Subscripts

a	air
b	base surface
m	porous media
o	initial state
r	reference state
sw	side walls
t	top surface
∞	surrounding

ACKNOWLEDGEMENTS

This research was supported by Shiraz University Research Council.

REFERENCES

1. K. J. Beukema and S. Bruin; *Int. J. of Heat and Mass Transfer*; 26,451 (1983).
2. M. Treiterer; *Int. J. of Heat and Mass Transfer*; 20,1045 (1977).
3. A. Zebib and D. R. Kassoy; *Physics of Fluids*; 21,1 (1976).
4. K. Aziz and J. D. Hellumes; *Physics of Fluids*; 10,314 (1967).
5. D. W. Peaceman and H. H. Rachford; *J. Soc. Indust. Appl. Math.*; 3 (1), 28 (1955).
6. K. Kublbeck, G. P. Merker and J. Straub; *Int. J. Heat Mass Transfer*, 23,203-217.
7. M. A. Yaghoubi and F. P. Incropera; *Numerical Heat Transfer*, 3, 315, (1980).
8. P. Vasseur, M. G. Satish and L. Robillard; "Natural Convection in a Thin Inclined Porous Layer Exposed to a Constant Heat Flux", *Proceedings of Heat Transfer Conference, San Francisco, CA U.S.A.*; Vol. 5, PP 2665-2670 (1985).
9. A. S. Householder "The Theory of Matrices in Numerical Analysis"; Blaisdell, New York.
10. M. N. Ozisik; "Heat Conduction"; John Wiley and Sons, Inc.
11. Gh. Karimi; "Computer Simulation of Natural Convection Heat Transfer in Porous Media with Internal Heat Generation Sources", M. S. Thesis (1989).